



OPEN

Polar amplification comparison among Earth's three poles under different socioeconomic scenarios from CMIP6 surface air temperature

Aihong Xie¹, Jiangping Zhu^{1,2}, Shichang Kang¹, Xiang Qin¹, Bing Xu^{1,2} & Yicheng Wang³

The polar amplification (PA) has become the focus of climate change. However, there are seldom comparisons of amplification among Earth's three poles of Arctic (latitude higher than 60°N), Antarctica (Antarctic Ice Sheet) and the Third Pole (the High Mountain Asia with the elevation higher than 4000 m) under different socioeconomic scenarios. Based on CMIP6 multi-model ensemble, two types of PA index (PAI) have been defined to quantify the PA intensity and variations, and PAI1/PAI2 is defined as the ratio of the absolute value of surface air temperature linear trend over Earth's three poles and that for global mean/over other regions except Earth's three poles. Arctic warms fastest in winter and weakest in summer, followed by the Third Pole, and Antarctica warms least. The similar phenomenon proceeds when global warming of 1.5–2.0 °C, and 2.0–3.0 °C above pre-industrial levels. After removing the Earth's three poles self-influence, all the PAI2s increase much more obviously relative to the PAI1s, especially the Antarctic PAI. Earth's three poles warm faster than the other regions. With the forcing increasing, PA accelerates much more over Antarctica and the Third Pole, but becomes weaker over Arctic. This demonstrates that future warming rate might make a large difference among Earth's three poles under different scenarios.

With the introduction of the Third Pole¹, the Arctic, Antarctica and the Third Pole have been collectively referred to as the “three poles of the Earth”², and become a new focus of climate change research^{3,4}. Earth's three poles are sensitive to climate change², and also play an important role in climate system^{5,6}. The cryosphere melting from Earth's three poles makes an outstanding contribution to sea-level rise with the glacier, snow cover, sea ice and ice sheet experiencing a widespread and conspicuous shrinking during the last decades^{5,7–10}.

Surface air temperature (SAT) plays a vital role in the cryosphere melting of Earth's three poles with the unprecedented global warming^{9,11}. Each of the last four decades has been successively warmer than any decade since 1850¹¹. Global SAT was 0.99 °C higher in 2001–2020, and 1.09 °C higher in 2011–2020 than 1850–1900, with larger increases over land (1.59 °C) than over ocean (0.88 °C)¹¹. Earth's three poles exhibit the different temperature variations². The Arctic region including Arctic Ocean has warmed two to four times as fast as the global average over the last few decades, commonly known as Arctic amplification (AA)^{8,12,13}. Different from the Arctic homogeneous warming, Antarctic temperature change is more complicated, with the general characteristic of faster warming in Antarctic Peninsula and West Antarctica than in East Antarctica^{14,15} and even with the regional warming absent^{16,17}. The strong warming in high-elevation regions is an intrinsic feature of recent global warming¹⁸, and the warming magnitude over the Third Pole is smaller than that over high latitudes in the northern hemisphere^{19,20}, but larger than Southern Hemisphere and tropics²¹.

The conspicuous increase of Greenland Ice Sheet melting and its contribution to sea level rise in the future is largely determined by the intensity of Arctic amplification and the global equilibrium climate sensitivity^{10,22,23}. As a robust feature of polar warming seen in historical observations and climate model simulations, polar amplification has been doubtful for the mechanism. Besides the natural climate variability, polar amplification in recent decades mainly contributes to the positive local lapse-rate feedback²⁴, including ice-albedo and Planck

¹State Key Laboratory of Cryospheric Sciences, Northwest Institute of Eco-Environment and Resources, Chinese Academy of Sciences, Lanzhou, China. ²University of Chinese Academy of Sciences, Beijing, China. ³Lanzhou Central Meteorological Observatory, Lanzhou, China. ✉email: zhujiangping@nieer.ac.cn

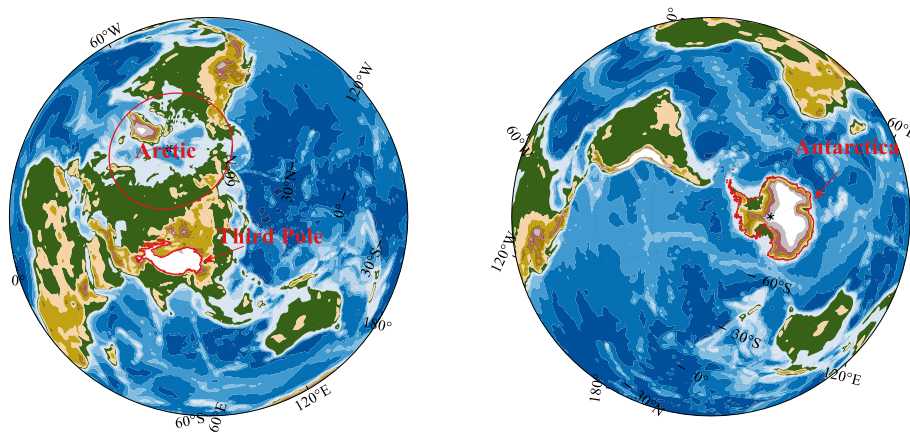


Figure 1. The locations of the Earth's three poles. The map was drawn in the software MATLAB R2018b (<https://ww2.mathworks.cn/products/matlab.html>).

feedbacks acting as supporting roles²⁵, downward clear-sky longwave feedbacks, and surface albedo feedback^{2,26}, etc. Accurate predictions of polar warming are critical given the fundamental role that polar ice plays in climate system, terrestrial and marine ecosystems, and human society^{2,7}. However, comparison research on the amplification of Earth's three poles has still been scarce. Therefore, our goal is (1) to compare the amplification variation of Earth's three poles during 2015–2100, with the CMIP6 multi-model outputs under different socioeconomic pathways (SSPs) of SSP1-1.9, SSP1-2.6, SSP2-4.5, SSP3-7.0 and SSP5-8.5, and under global warming of 1.5 °C, 2.0 °C and 3.0 °C above pre-industrial levels; (2) to quantify and compare the pole amplification with other regions during 2015–2100 through different polar amplification indices (PAIs).

Data and methods

Data sources. The Coupled Model Intercomparison Project (CMIP) works to better understand the past, present and future climate change caused by natural and unforced variability²⁷. In the CMIP6 latest-generation climate models, one third exhibits the higher equilibrium climate sensitivity²⁸, and a new set of alternative pathways of future societal development are described as shared socioeconomic pathways (SSPs) of future radiative forcing used for sustainable development problems analysis²⁹. Forcings are provided by the integrated assessment model for the future scenarios in Scenario Model Intercomparison Project (ScenarioMIP), harmonized with atmospheric emissions, concentrations and land use⁵⁷. The ScenarioMIP climate models from CMIP6 under the five SSPs of SSP1-1.9, SSP1-2.6, SSP2-4.5, SSP3-7.0, and SSP5-8.5 that cover the range of possible future development of anthropogenic drivers of climate change found in the literature¹¹, and the five socioeconomic scenarios are used to assess the surface air temperature change of Earth's three poles in twenty-first century. For the limit of CMIP6 model outputs in SSP1-1.9, we only use seven models (Table S3) to analyze the climate change during the period 2015–2100. The model outputs from the CMIP6 “historical” experiments cover the period 1850–2014, and are driven by observed boundary conditions³⁰.

Study area. This study focuses on the different extent for the three poles, and the locations of the three poles are shown in Fig. 1. The Arctic refers to the region that latitude higher than 60°N⁵, Antarctica refers to the Antarctic Ice Sheet, and the Third Pole is the High Mountain Asia with the average elevation more than 4000 m, including the highest and most spatially extensive highland in the world^{27,31}.

Definition of amplification index. Polar amplification is commonly defined as the ratio of polar warming to tropical warming, which can estimate the robust feature of climate change²⁵. To quantitate the amplification over Earth's three poles, the polar amplification index (PAI) has been defined as the ratio of the absolute value of surface atmosphere temperature (SAT) linear trend over Earth's three poles and that for global mean (PAI1). To eliminate the self-influence from the loop computation of the three poles, this study has also defined one other PAI as the ratio of the SAT trend over Earth's three poles and that over other regions except Earth's three poles (PAI2), to further compare the warming between Earth's three poles and other regions.

Calculation from CMIP6 data. To uniform the resolution from different models, the scenario data are regridded into the resolution of 0.25° × 0.25° using the bilinear interpolation. With considering uncertainties, the multi-model ensemble mean (MMEM) is an appropriate way for the model outputs, which weighs all models equally^{20,32}. ERA5 is the latest atmospheric reanalysis produced by European Centre for Medium-Range Weather Forecasts (ECMWF), and it has high skill in representing the temperature across the Earth's three poles^{33–35}. Generally, temperature from the MMEM can capture the spatial patterns over the Arctic, Antarctica and the Third Pole, although the bias inevitably exists (Fig. 2).

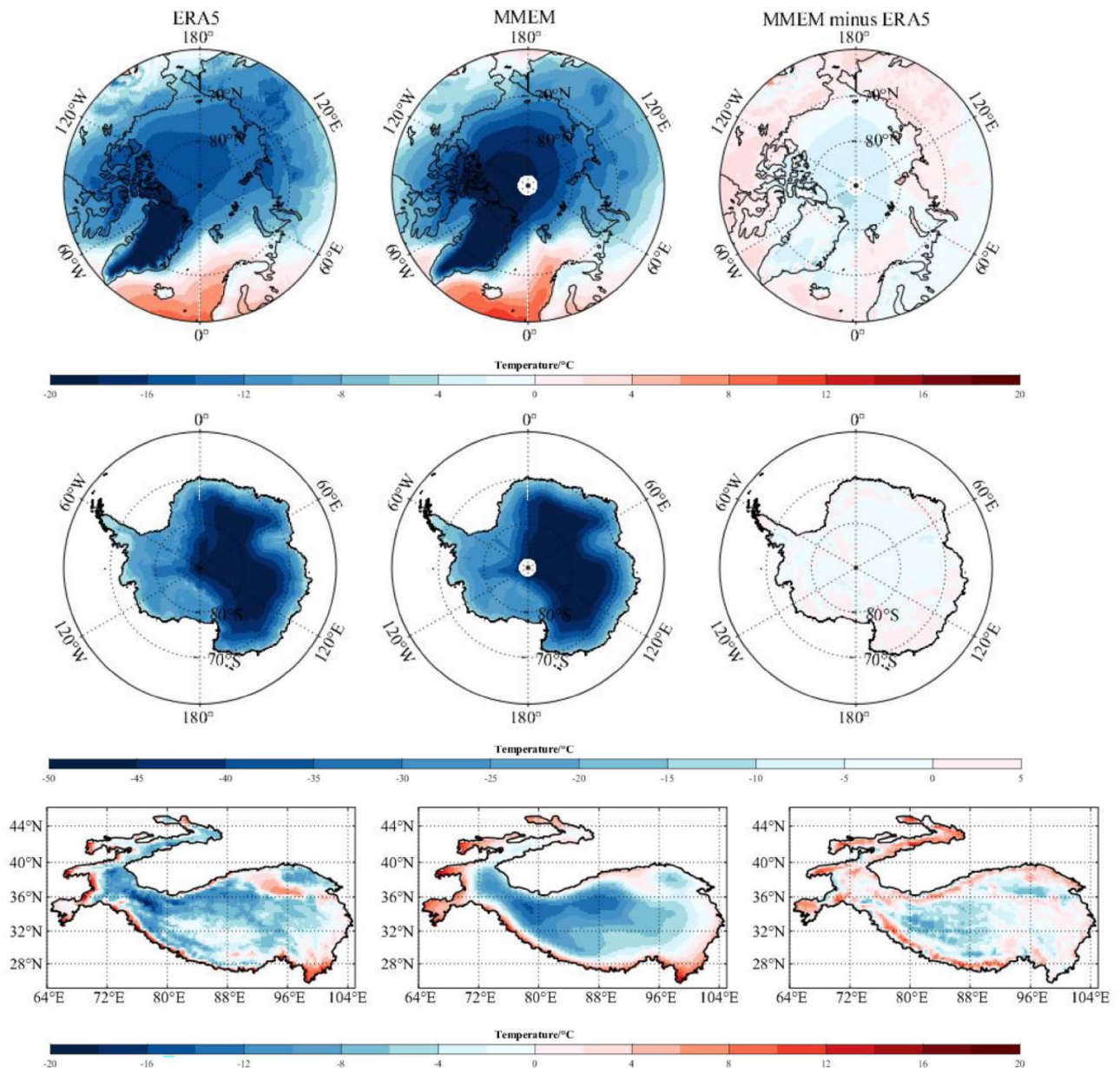


Figure 2. Spatial patterns of annual mean temperature from the ERA5 (left panel), the multi-model ensemble mean (MMEM) of the CMIP6 model simulations (center panel), and their biases (MMEM minus ERA5) (right panel) over the Arctic, Antarctica and The Third Pole during 1979–2014. The map was drawn in the software MATLAB R2018b (<https://ww2.mathworks.cn/products/matlab.html>).

We have employed the simple linear regression to calculate the trend of temperature, and the regression procedure chooses the line producing the least error³⁶, and F test is used to estimate the significance ($p < 0.05$) of temperature trends. For the regional mean, the temperature is calculated by simply averaging the grid data in the area, and further obtain the regional trend and calculate the regional PAI. Similarly, the spatial analysis of trend is based on a simple regression of the temperature at each grid point. The spatial distribution of the PAI1/PAI2 is the absolute ratio of the grid temperature trend to the global average temperature trend/the trend over the other regions except Earth's three poles.

Results

Amplification comparison among Earth's three poles under different socioeconomic scenarios. The time series in Fig. 3 shows the annual surface air temperature anomaly relative to the 1850–1900 baseline period over the Arctic, Antarctica, the Third Pole and global mean during the period 1850–2100 from MMEM under different SSPs of SSP1-1.9, SSP1-2.6, SSP2-4.5, SSP3-7.0 and SSP5-8.5. The annual temperature over the Arctic and the Third Pole obviously increases faster than global mean, especially in the high forcing socioeconomic scenarios. Under SSP5-8.5, the global mean will rise by approximately 6.0 °C at the end of

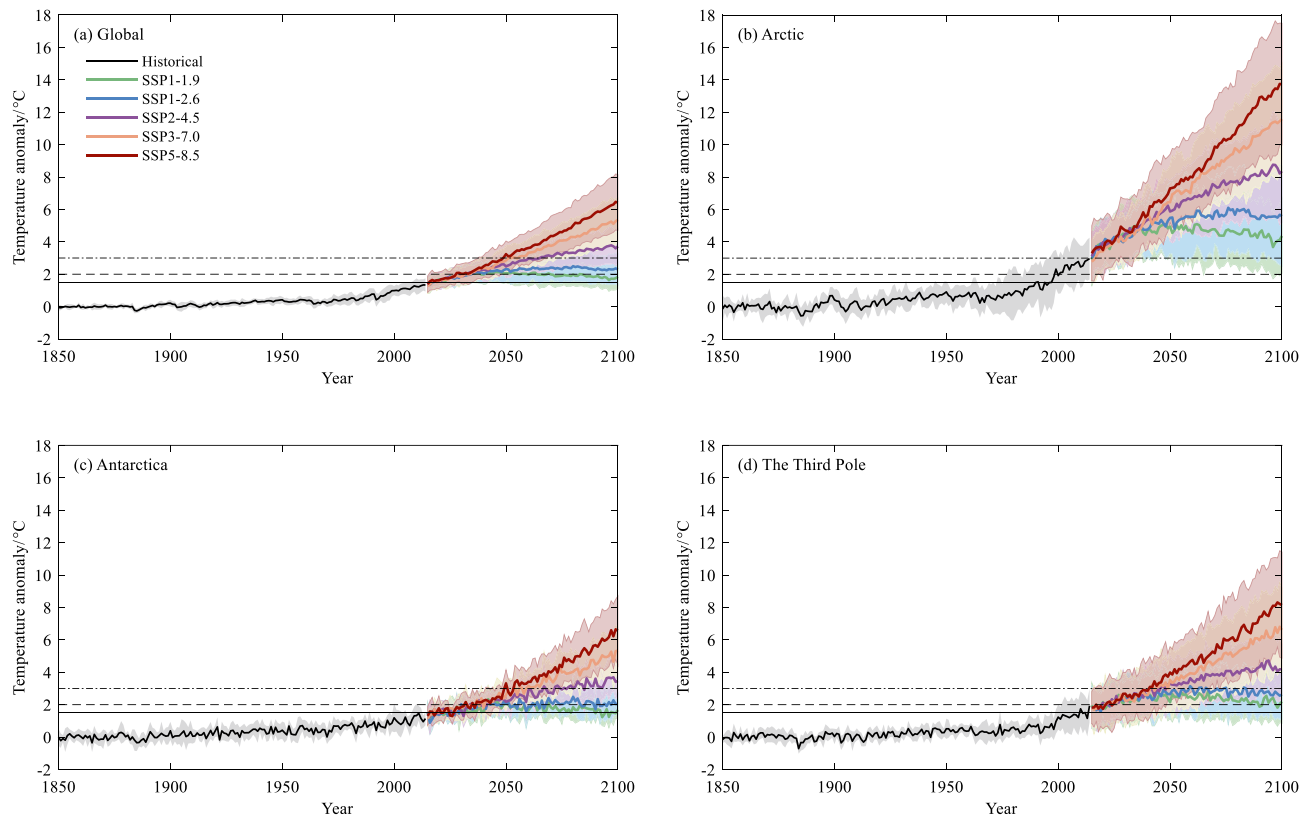


Figure 3. Annual mean surface air temperature anomaly ($^{\circ}\text{C}$, 1850–1900 as the baseline period) for (a) Global, (b) Arctic, (c) Antarctica and (d) The Third Pole during 1850–2100 from multi-model ensemble mean (MEM) of the CMIP6 simulations under the historical (black curve), SSP1-1.9 (green), SSP1-2.6 (blue), SSP2-4.5 (purple), SSP3-7.0 (orange), SSP5-8.5 (bronze/crimson), respectively. The black straight lines are for 1.5 $^{\circ}\text{C}$ (solid line), 2.0 $^{\circ}\text{C}$ (break line), 3.0 $^{\circ}\text{C}$ (breakpoint line), respectively.

twenty-first century, and the increase over the Arctic and the Third Pole are higher than 8.0 $^{\circ}\text{C}$, which indicates the occurrence of amplification and is consistent with the previous research^{37, 38}, whereas the signal is weak in Antarctica. The Arctic warming is most conspicuous among Earth's three poles. Even under SSP1-1.9 socio-economic scenario, Arctic warms more than 3.0 $^{\circ}\text{C}$. However, the Antarctic temperature rises lower than 2.0 $^{\circ}\text{C}$ in the SSPs of SSP1-1.9 and SSP1-2.6. Similar to annual mean, the three poles exhibit different sensitivity to future forcing. Global mean temperature shows the strong warming in DJF (December–February) except under SSP1-1.9 (Fig. 4). Under SSP3-7.0 and SSP5-8.5, Arctic will experience further warming of at least 17 $^{\circ}\text{C}$ in DJF compared with the 1850–1900 baseline by the end of the twenty-first century. Similarly, the greatest seasonal variability of Antarctic temperature occurs in winter JJA (June–August), with the warming anomaly of 6.34 $^{\circ}\text{C}$ under SSP5-8.5. Projections show that the most conspicuous warming of the Third Pole occurs in SON (September–November), ranging from 3.00 $^{\circ}\text{C}$ under SSP1-1.9 to 10.04 $^{\circ}\text{C}$ under SSP5-8.5 in 2100 relative to the baseline period.

The distribution of annual temperature trend under different SSPs over Earth's three poles during the period 2015–2100 is shown in Fig. 5. Obviously, the strongest warming occurs over the Arctic in all SSPs. Over large parts of the Arctic, annual mean temperatures increase higher than 1.0 $^{\circ}\text{C}$ per decade for the high-emission SSPs of SSP3-7.0 and SSP5-8.5. The conspicuous Arctic warming exceeds 2.0 $^{\circ}\text{C}$ per decade in DJF (not shown). Antarctic temperature shows the significantly positive trends over almost all grids, while the trends are generally weaker than Arctic and the Third Pole. MEM reveals conspicuous warming in JJA, especially over the Antarctic coast region. Over the Third Pole, faster warming concentrates on the northern Tibet Plateau under high-emission SSPs of SSP3-7.0 and SSP5-8.5. The strongest changing sign occurs in autumn over the Third Pole, with the warming above 1.0 $^{\circ}\text{C}$ per decade in SSP5-8.5. Among Earth's three poles, there is a broad consistency of warming signal in the future, with the strongest positive trends in Arctic and weakest in Antarctica.

To further explore the temperature changes over Earth's three poles, we calculate the trend of regional average for surface seasonal and annual temperature mean during 2015–2100 (Fig. 6). In all SSPs, Arctic performs the greatest increases, and the largest positive trend in DJF, with the rate of 0.05 $^{\circ}\text{C}$, 0.37 $^{\circ}\text{C}$, 0.94 $^{\circ}\text{C}$, 1.56 $^{\circ}\text{C}$ and 1.86 $^{\circ}\text{C}$ per decade under SSPs of SSP1-1.9, SSP1-2.6, SSP2-4.5, SSP3-7.0 and SSP5-8.5, respectively. However, the Antarctic warming is rather weak with the trend of almost below 0.69 $^{\circ}\text{C}$ per decade, and even a negative trend occurs in austral winter JJA under SSP1-1.9. Over the Third Pole, conspicuous warming trend appears in SON, with the rate ranging from 0.02 $^{\circ}\text{C}$ under SSP1-1.9 to 0.97 $^{\circ}\text{C}$ under SSP5-8.5.

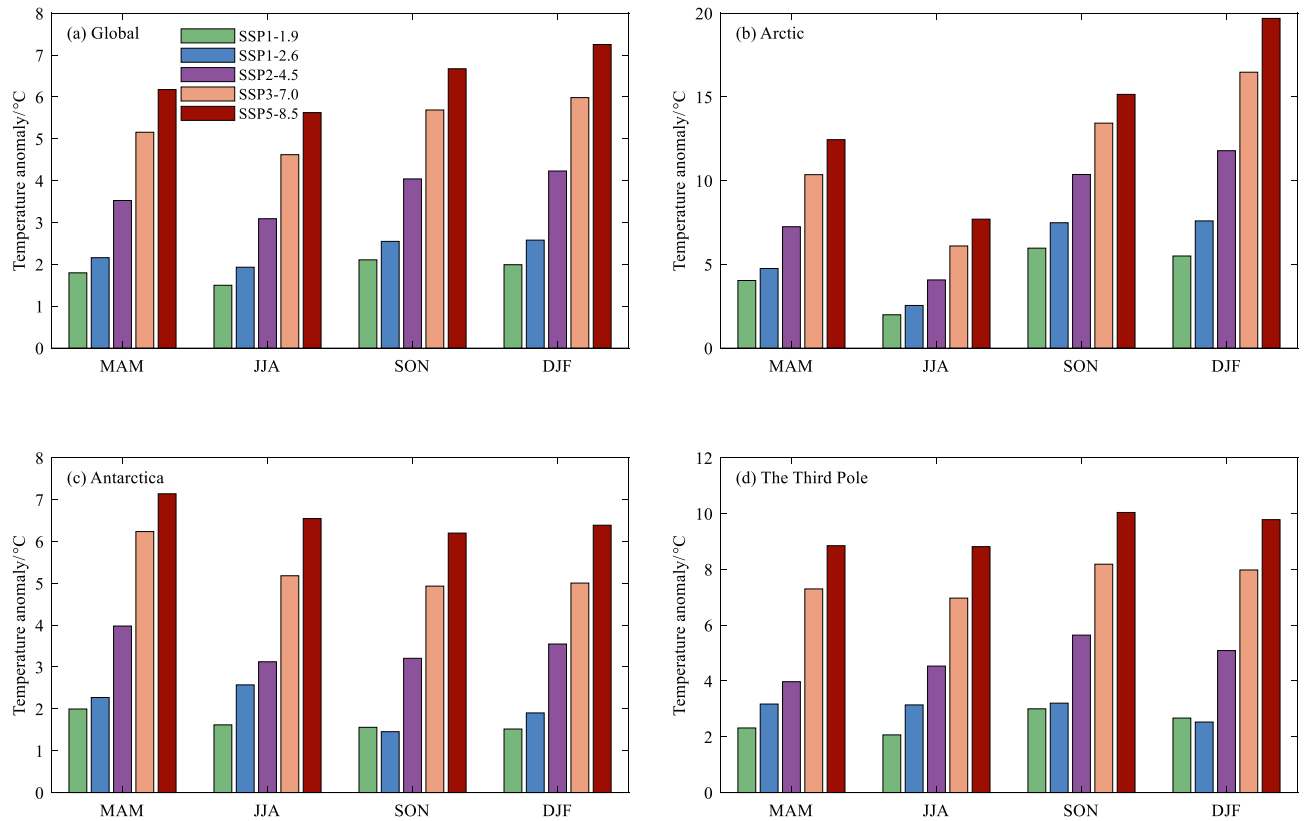


Figure 4. Surface air temperature anomaly ($^{\circ}\text{C}$, 1850–1900 as the baseline period) for seasonal mean for (a) Global, (b) Arctic, (c) Antarctica and (d) The Third Pole in 2100 from multi-model ensemble mean (MEM) of the CMIP6 simulations under SSP1-1.9 (green), SSP1-2.6 (blue), SSP2-4.5 (purple), SSP3-7.0 (orange), SSP5-8.5 (bronze), respectively. The season mean is from the three monthly average of MAM (March–May), JJA (June–August), SON (September–November) and DJF (December–February), respectively.

Amplification comparison among Earth’s three poles under the global warming of 1.5 $^{\circ}\text{C}$, 2.0 $^{\circ}\text{C}$ and 3.0 $^{\circ}\text{C}$. The Paris Agreement of the United Nations Framework Convention on Climate Change (UNFCCC) sets a goal to limit the increase of global mean temperature to “well below 2 $^{\circ}\text{C}$ ” and fights to limit warming to 1.5 $^{\circ}\text{C}$ relative to pre-industrial level³⁹. Many researches aim to compare the changes under the global warming of 1.5 $^{\circ}\text{C}$, 2.0 $^{\circ}\text{C}$ and 3.0 $^{\circ}\text{C}$ above pre-industrial levels, and/or examine whether a lower target warming is necessary^{27, 40}. Global warming of 1.5 $^{\circ}\text{C}$ and 2.0 $^{\circ}\text{C}$ period is defined to be the time when the global average surface air temperature anomaly is 1.3–1.7 $^{\circ}\text{C}$ and 1.8–2.2 $^{\circ}\text{C}$ warmer relative to the pre-industrial period (1850–1900), respectively^{27, 41}. To explore the temperature changes of Earth’s three poles in different thresholds, we calculate the regional temperature changes when global warming is from 1.5 $^{\circ}\text{C}$ to 2.0 $^{\circ}\text{C}$. Under SSP1-1.9 the 2.0 $^{\circ}\text{C}$ warming is not possible and is omitted there.

When global mean warms from the 1.5 $^{\circ}\text{C}$ to 2.0 $^{\circ}\text{C}$ threshold, the increase of Arctic temperature is higher than 0.5 $^{\circ}\text{C}$ except in summer JJA, and annual mean warms 1.07 $^{\circ}\text{C}$, 0.85 $^{\circ}\text{C}$, 0.92 $^{\circ}\text{C}$ and 1.08 $^{\circ}\text{C}$ in SSP1-2.6, SSP2-4.5, SSP3-7.0 and SSP5-8.5 (Table S1), respectively. The change of Arctic temperature is conspicuous in autumn and winter, with the increase of 1.47 $^{\circ}\text{C}$, 1.18 $^{\circ}\text{C}$, 1.21 $^{\circ}\text{C}$ and 1.43 $^{\circ}\text{C}$ in SON from the lower forcing to the highest, and the corresponding value in DJF is 1.54 $^{\circ}\text{C}$, 1.26 $^{\circ}\text{C}$, 1.25 $^{\circ}\text{C}$ and 1.42 $^{\circ}\text{C}$, respectively. Not surprisingly, Antarctica exhibits the slowest warming among Earth’s three poles, and even though Antarctic fails to warm 0.50 $^{\circ}\text{C}$ in austral winter JJA. For the Third Pole, annual mean successfully warms faster than global in all SSPs, and the strong warming signal occurs in autumn and winter.

When global mean warms from the 1.5 $^{\circ}\text{C}$ to 2.0 $^{\circ}\text{C}$ threshold, the annual warming of Earth’s three poles is obvious in SSP1-2.6 and SSP5-8.5 in general (Table S1), and these SSPs also represent the extreme forcing. Therefore, we only illustrate the distribution of annual temperature changing when global warming by 0.50 $^{\circ}\text{C}$ under these SSPs (Fig. 7). Clearly, most of Arctic regions warm faster than global, even some region warms more than twice as fast as the global average. The annual warming higher than 0.5 $^{\circ}\text{C}$ concentrates on the interior of East Antarctica in SSP1-2.6, and the most profound warming occurs in DJF. With the similar character in Arctic, the increase of the Third Pole temperature is also conspicuous in SON and DJF. Compared with Arctic, faster warming in the Third Pole can be found in JJA, with the increase of 0.82 $^{\circ}\text{C}$, 0.50 $^{\circ}\text{C}$, 0.49 $^{\circ}\text{C}$ and 0.79 $^{\circ}\text{C}$ under SSP1-2.6, SSP2-4.5, SSP3-7.0 and SSP5-8.5.

When global mean warms from 2.0 $^{\circ}\text{C}$ to 3.0 $^{\circ}\text{C}$, the annual temperature mean over the Antarctica fails to achieve the 1.0 $^{\circ}\text{C}$ warming under the SSPs of SSP2-4.5, SSP3-7.0 and SSP5-8.5 (Table S2). In stark contrast, the strong warming of Arctic and the Third Pole can be observed, with the rise of annual mean exceeds 1.3 $^{\circ}\text{C}$. For

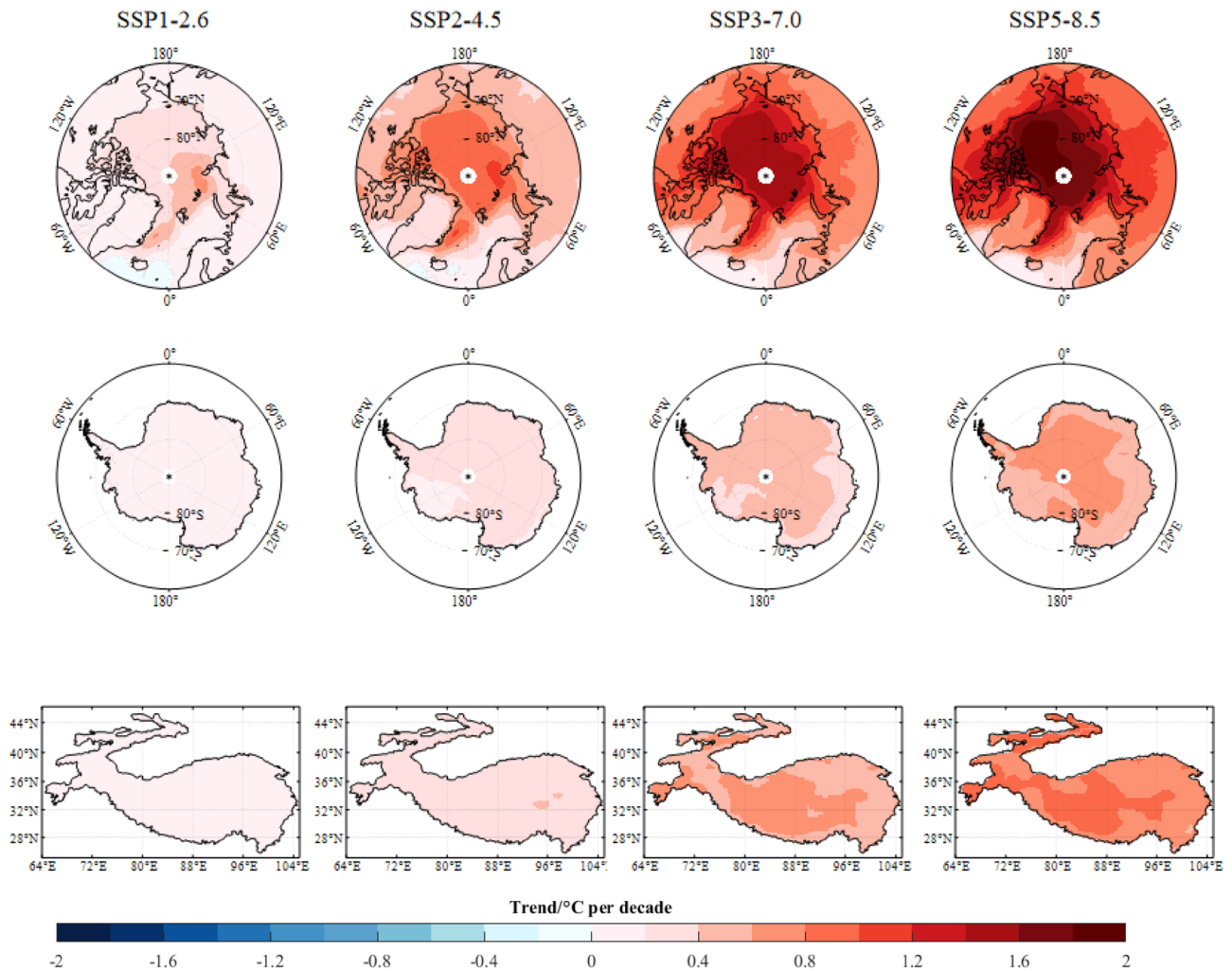


Figure 5. Spatial patterns of annual temperature trend over the Arctic, Antarctica and The Third Pole from the multi-model ensemble mean (MME) of the CMIP6 simulations under different SSPs during 2015–2100. The grey dotted region represents that the trend is not significant. The map was drawn in the software MATLAB R2018b (<https://ww2.mathworks.cn/products/matlab.html>).

Arctic, the conspicuous warming occurs in DJF, with the increase of 3.65 °C, 3.93 °C and 3.45 °C from middle to the highest forcing. For the Third Pole, the changes of temperature exaggerate with the forcing increasing except in summer JJA.

Amplification Quantification over Earth's three poles through PAI1 under different socio-economic scenarios. The zonal mean temperature trends averaged from latitude circles for annual and seasonal mean under different SSPs is shown in Fig. 8. Inevitably, the strong AA can be captured in all cases. The zonal mean trend increases poleward to Arctic, with exception in JJA, and the phenomenon is symmetry in Antarctica. Generally, the zonal trend over Antarctica is higher than that of middle and low latitudes in southern hemisphere. However, the latitude effect is weaker than northern hemisphere. The meridional average trend only for the Third Pole region presents the faster change than the zonal mean, and it indicates the appearance of Third Pole amplification (TA).

Compared with the global mean, Earth's three poles amplification index (PAI1) has been provided in Table 1, as the ratio of the absolute value of SAT linear trend over Earth's three poles and that for global mean. Table 1 quantifies the annual and seasonal variations in different SSPs, but excludes SSP1-1.9 socioeconomic scenario, since the SSP1-1.9 mean trend is too low to cause the index incredibility. Arctic amplification always exists with the annual warming PAI1 of 2.76, 2.29, 2.21 and 2.11 times than global mean under SSP1-2.6, SSP2-4.5, SSP3-7.0 and SSP5-8.5, respectively. In accordance with the annual mean rapid warming, the AA is most conspicuous in DJF, with the AA index of 3.39, 2.93, 2.86 and 2.73 under SSP1-2.6, SSP2-4.5, SSP3-7.0 and SSP5-8.5, respectively. However, Table 1 illustrates that Arctic Amplification might decelerate with the increase of radiative forcing from the low to high SSPs, except in summer JJA. Much weaker than AA, annual AnA doesn't exist with the annual PAI1 lower than 1 except in SSP5-8.5. AnA also displays the seasonal variations, with all the PAI1 higher than 1 only in autumn MAM, and all the PAI1 lower than 1 in spring SON and summer DJF. Different from AA, TA

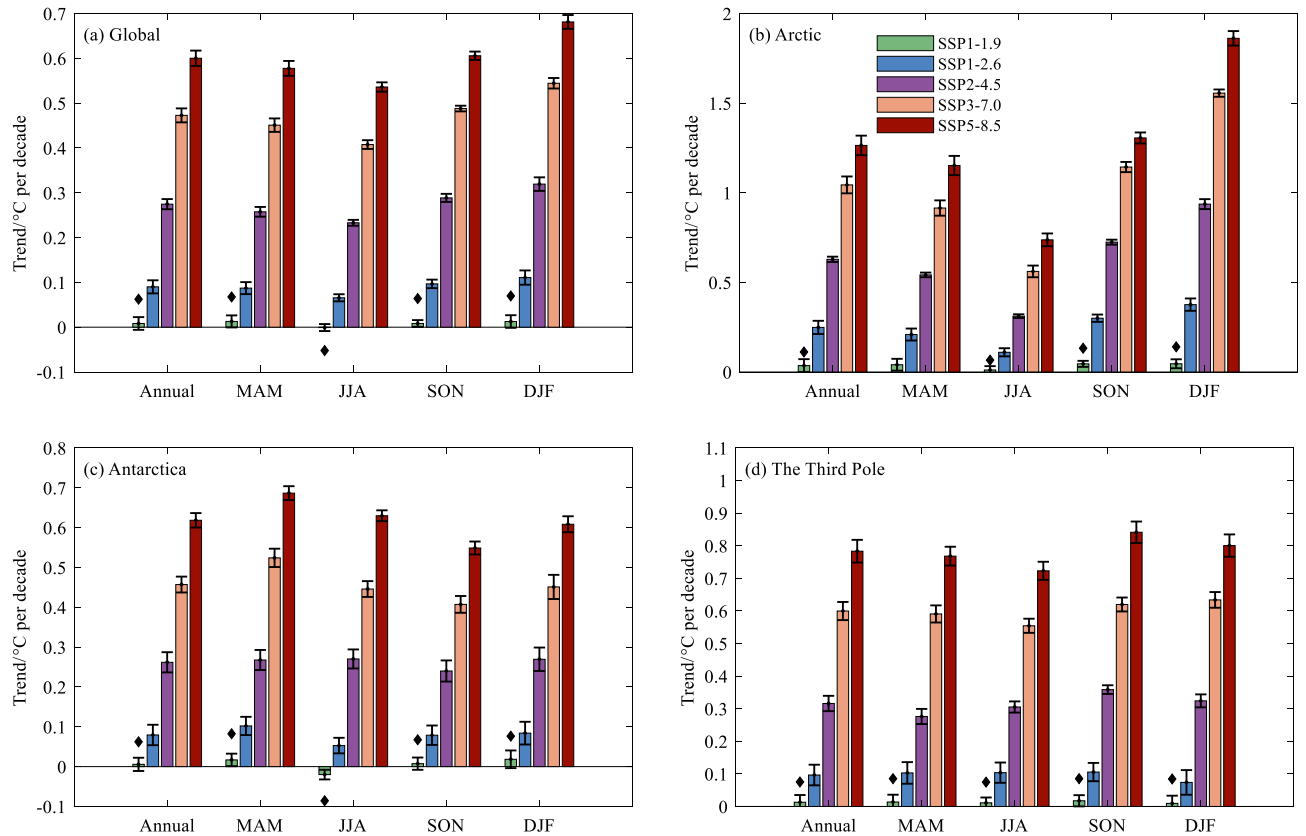


Figure 6. Similar to Fig. 4, but for regional average trends (°C per decade) during 2015–2100. The black rhombus symbol \blacklozenge represents that the trend is not significant. The others are significant at the 95% confidence interval.

enhances with the increase of forcing from the low to high socioeconomic scenarios. Much larger than AnA, TA dominates the whole year, especially in JJA and SON, with the amplification index higher than 1.20 in general.

To better understand the amplification in Earth's three poles, spatial patterns of amplification index for annual temperature is shown in Fig. 9. Arctic high amplification index concentrates near the North Pole in general. The Antarctic amplification always occurs in East Antarctic inland, and disappears in the Antarctic coast and West Antarctica. The polar amplification dominates the Third Pole, only except the southeast region. For Antarctica, the amplification is most extensive in MAM and JJA (not shown), and the index is lower than 2 in general. Generally, the distribution of amplification index over the Third Pole is uniform, with the value between 1 and 2. Contrary to the conspicuous Arctic amplification in DJF, majority of the region from the Third Pole fails to achieve amplification under the SSP1-2.6 socioeconomic scenario.

Polar amplification compared with other regions under different socioeconomic scenarios. The above research suggests that Earth's three poles generally warm faster than the global mean warming. To further explore the polar amplification compared with the other regions, this study has also defined one other new polar amplification index (PAI2), as the ratio of the SAT trend over Earth's three poles and that over other regions except the Earth's three poles, which can eliminate the self-influence from the Earth's three poles. Table 2 lists the new index, and Fig. 10 shows the corresponding spatial patterns for the three poles amplification, respectively.

Compared with PAI1, PAI2 shows that the PA obviously enhances more sharply from Fig. 10 and Table 2 than that from Fig. 9 and Table 1, and the polar warming is conspicuously faster than the other regions of global mean under all SSPs. Especially for Arctic in DJF, the AA index is more than 4 and even up to 6. Even in Antarctica, almost all the indexes are above 1.0, only except for austral winter in SSP1-2.6 scenario. Similar to the previous index PAI1 from Table 1, the AA from Table 2 is the most conspicuous among the Earth's three poles, and the strongest AA occurs in winter, with all PAI2 index over the Arctic Ocean almost more than 4 in DJF. The weakest AA is in JJA with the PAI2 of 1.90 in SSP1-2.6. In general, Arctic is from 1.5 to 6.3 times the global mean after eliminating Earth's three poles mean warming. The AA becomes weaker from SSP1-2.6 to SSP5-8.5, with exception of JJA. Differently from PAI1, PAI2 illustrates that the AnA index (Table 2) displays the obvious seasonal variations, and increases highest in austral autumn, with index values of 1.76, 1.38, 1.54 and 1.57 in SSP1-2.6, SSP2-4.5, SSP3-7.0 and SSP5-8.5, respectively. However, the coastal of the East Antarctica always miss the amplification signal in austral summer DJF in all SSPs (not shown). In addition, Antarctic Peninsula rarely illustrates the amplification in austral spring SON and summer DJF, with exception of the SSP5-8.5. Similar to

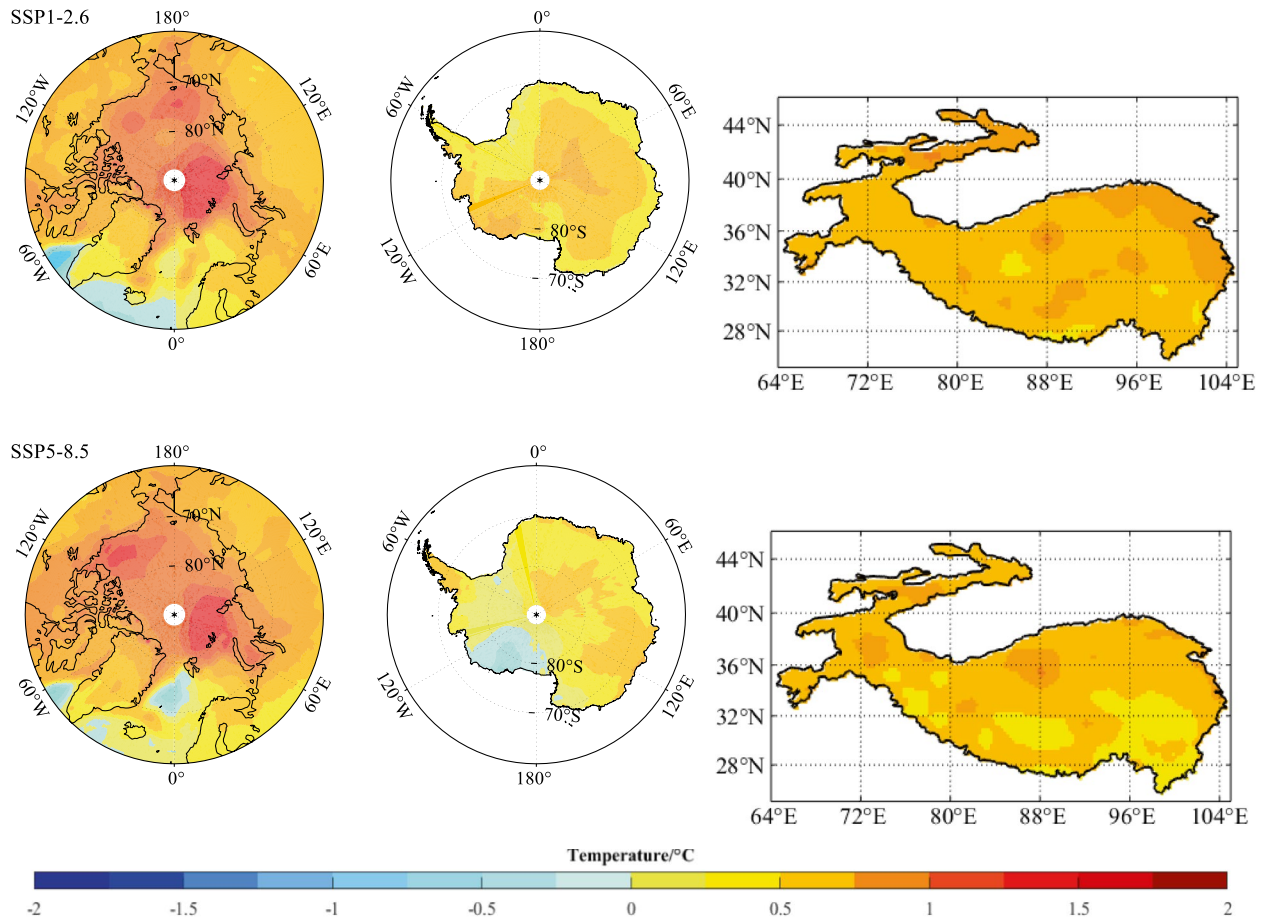


Figure 7. Spatial patterns of annual mean temperature difference (°C) over Arctic, Antarctica and The Third Pole from the CMIP6 simulations MMEM when global warming reaches 1.5 °C and 2.0 °C threshold above pre-industrial levels only under SSP1-2.6 and SSP5-8.5. The map was drawn in the software MATLAB R2018b (<https://ww2.mathworks.cn/products/matlab.html>).

PAI1, PAI2 shows that the most conspicuous warming occurs in autumn SON over the Third Pole, with the PAI2 of 1.86, 1.76, 1.71 and 1.81 under SSP1-2.6, SSP2-4.5, SSP3-7.0 and SSP5-8.5, respectively. The amplification dominates the Third Pole in all socioeconomic scenarios, and becomes much stronger in boreal autumn MAM and winter DJF. Similar to the PAI1, PAI2 also demonstrates and exaggerates that the intensity of AA generally decreases from SSP1-2.6 to SSP5-8.5, whereas the amplification over Antarctica and the Third Pole has a distinct accelerating tendency with the increase of forcing.

Discussions

The climate sensitivity and inter-model spread of the past climate simulations may introduce uncertainty into the projection of future climate. Compared to CMIP5, the CMIP6 models show a higher average climate sensitivity, and the CMIP6 models tend to overestimate the trend of global mean surface temperature^{11,42}. In addition, we calculate the trend using the simple linear regression, but not consider serial correlation effect of the temperature time series, and the trends should be narrower than the real expected values⁴³. Most climate models fail to represent the amplitude of polar temperature change observed in paleoclimatic archives, which relates to the underestimation of aerosols effect on polar regions, and this bias may influence future predictions⁴⁴. Surface albedo, water vapor feedbacks, atmospheric and oceanic heat transport are important processes to the warming of polar regions^{45,46}. Previous research has found that the ice-albedo feedback can be influenced by clouds, and one third of the models in CMIP6 refer to the cloud feedbacks inaccuracy, and the feedback strength depends on a large number of physical processes and parametrizations, which differs remarkably among the models³³. Compared with CMIP5, CMIP6 has reduced the models range, and shows better performance in representing the distribution of sea ice concentration⁴⁷. The Greenland Ice Sheet mass loss in CMIP6 equates to a CMIP5 scenario with twice the global radiative forcing¹⁰. Antarctic sea ice extent (SIE) has always been underestimated in austral summer³⁴. The CMIP6 MMEM can perform the seasonal cycles of the Arctic and Antarctic SIE, while it fails to represent the faster decline of Arctic SIE and the larger interannual variability in Antarctic SIE after 2000⁴⁸. CMIP6 MMEM can capture the climatological spatial distribution of Amundsen Sea Low, but underestimates the intensity⁴⁹. Over the Third Pole, CMIP6 models exhibit a warm temperature bias in summer and

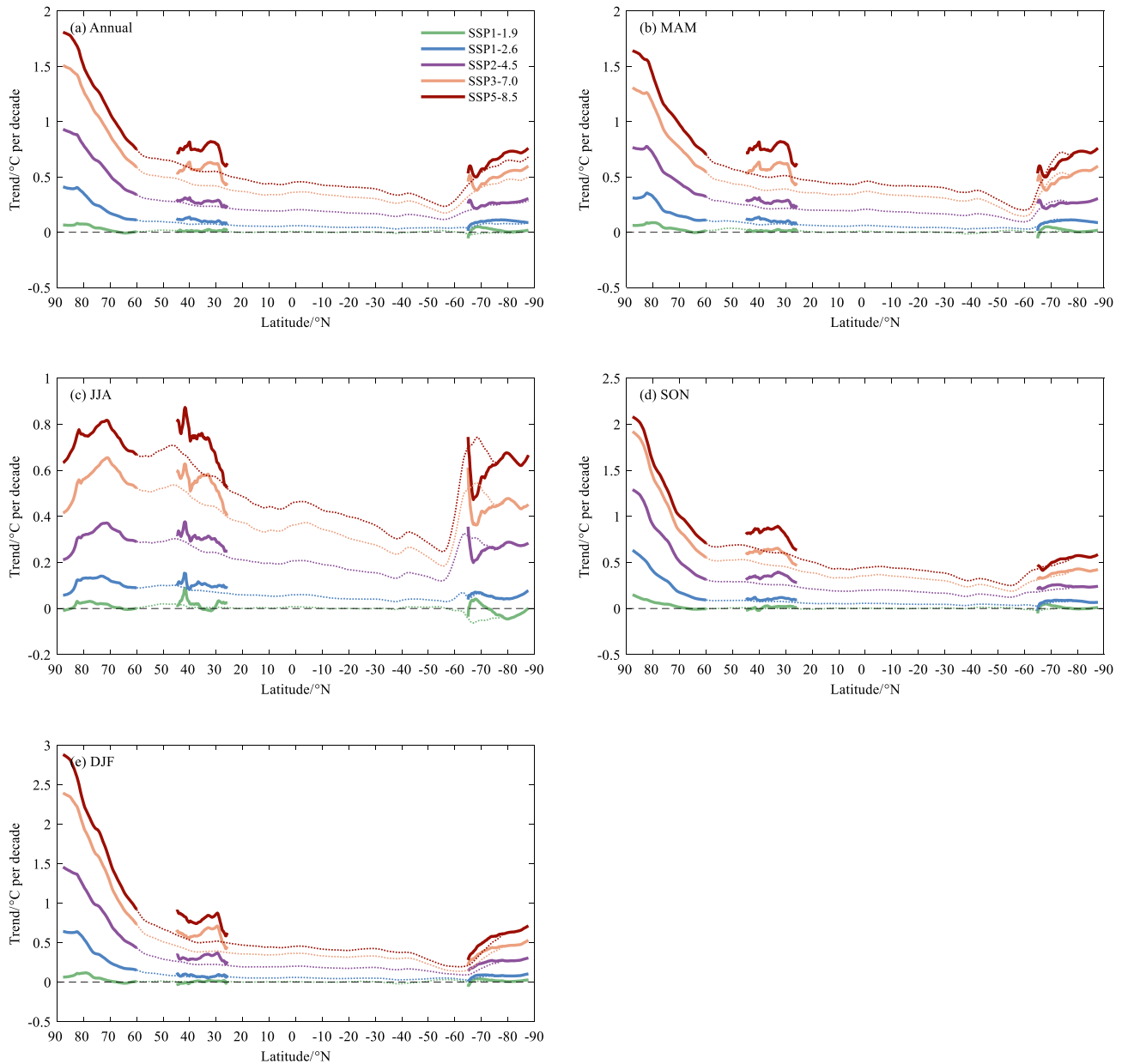


Figure 8. Zonally average temperature trends ($^{\circ}\text{C}$ per decade) for (a) annual and (b–e) seasonal during 2015–2100 from the CMIP6 simulations MMEM under the SSPs of SSP1-1.9, SSP1-2.6, SSP2-4.5, SSP3-7.0, SSP5-8.5, respectively. The dotted line is for the zonal average from latitude circles, and the solid is for the three poles.

cold bias in winter⁵⁰. Compared with the CMIP5 models, CMIP6 models perform generally better in the Third Pole⁵¹. The spring sensible heating over the Third Pole has important influence on the Asian summer monsoon, and the future outputs from CMIP6 confirms an increasing trend, and gets stronger with the increase of forcing from SSP1-2.6 to SSP5-8.5⁵².

Under different global warming thresholds, Arctic and Antarctica are both sensitive to the increase in atmospheric CO_2 concentration, and the strong warming occurs in Arctic in all socioeconomic scenarios⁵³. Similarly, the strong increase of Arctic temperature can be observed in all cases when global warming exceeds from 1.5 $^{\circ}\text{C}$ /2.0 $^{\circ}\text{C}$ to 2.0 $^{\circ}\text{C}$ /3.0 $^{\circ}\text{C}$ thresholds. For Antarctica, temperature increases basically consistent with the global mean under the 1.5 $^{\circ}\text{C}$ and 2.0 $^{\circ}\text{C}$ thresholds, whereas the strong local warming over Antarctica occurs when global warming exceeds 1.5 $^{\circ}\text{C}$ threshold⁴⁹. Consistently, the increase of temperature higher than 0.5 $^{\circ}\text{C}$ can be captured in some regions over East Antarctica when global mean warms from 1.5 $^{\circ}\text{C}$ to 2.0 $^{\circ}\text{C}$ threshold. For the Third Pole, it will achieve the 1.5 $^{\circ}\text{C}$ and 2.0 $^{\circ}\text{C}$ warming approximately 10 years earlier than the global scale⁵⁴. When global temperature rises by 0.5 $^{\circ}\text{C}$, the Third Pole exhibits the stronger warming in all socioeconomic scenarios.

The fastest Arctic warming occurs in DJF under all socioeconomic scenarios, which is identical with the previous estimation with CMIP5, which holds the point that Arctic warming is most pronounced in winter and

	Annual	MAM	JJA	SON	DJF
Arctic					
SSP1-2.6	2.76	2.40	1.68	3.11	3.39
SSP2-4.5	2.29	2.10	1.34	2.51	2.93
SSP3-7.0	2.21	2.03	1.38	2.34	2.86
SSP5-8.5	2.11	1.99	1.38	2.16	2.73
Antarctica					
SSP1-2.6	0.88	1.17	0.81	0.82	0.76
SSP2-4.5	0.95	1.04	1.16	0.83	0.84
SSP3-7.0	0.97	1.16	1.09	0.83	0.83
SSP5-8.5	1.03	1.19	1.18	0.91	0.89
The Third Pole					
SSP1-2.6	1.07	1.18	1.58	1.09	0.67
SSP2-4.5	1.15	1.07	1.31	1.24	1.01
SSP3-7.0	1.27	1.31	1.36	1.27	1.16
SSP5-8.5	1.31	1.33	1.35	1.39	1.18

Table 1. The Amplification Index (PAI1) based on global mean over Arctic, Antarctica, the Third Pole under SSP1-2.6, SSP2-4.5, SSP3-7.0 and SSP5-8.5, respectively.

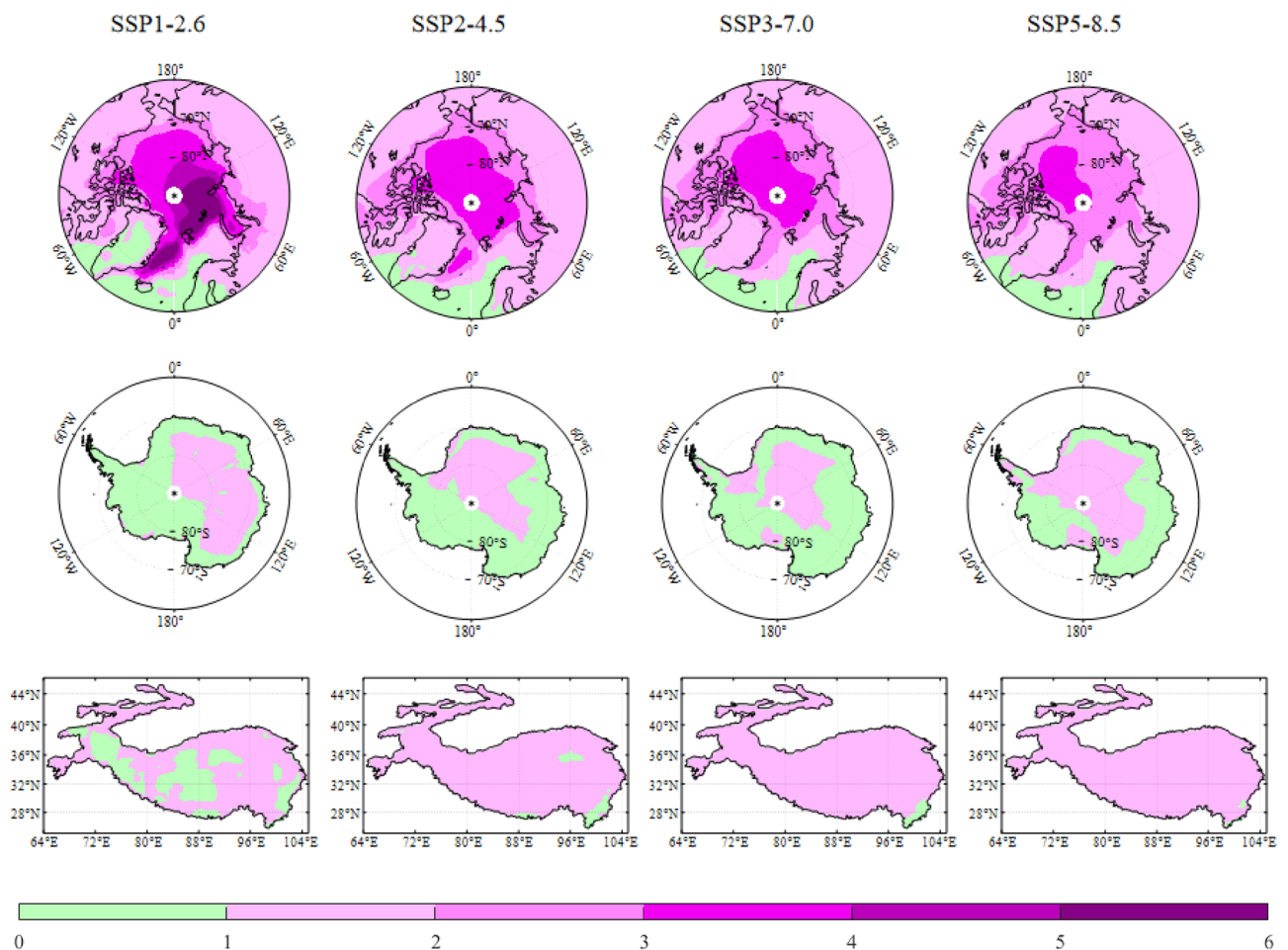


Figure 9. Similar to Fig. 5, but for the Polar amplification Index (PAI1) during 2015–2100. The map was drawn in the software MATLAB R2018b (<https://ww2.mathworks.cn/products/matlab.html>).

	Annual	MAM	JJA	SON	DJF
Arctic					
SSP1-2.6	4.29	3.60	1.90	5.28	6.32
SSP2-4.5	3.14	2.79	1.54	3.55	4.65
SSP3-7.0	2.96	2.69	1.58	3.16	4.39
SSP5-8.5	2.78	2.63	1.60	2.81	4.08
Antarctica					
SSP1-2.6	1.37	1.76	0.91	1.39	1.41
SSP2-4.5	1.31	1.38	1.34	1.18	1.34
SSP3-7.0	1.30	1.54	1.25	1.13	1.27
SSP5-8.5	1.36	1.57	1.37	1.18	1.34
The Third Pole					
SSP1-2.6	1.66	1.77	1.80	1.86	1.24
SSP2-4.5	1.58	1.42	1.51	1.76	1.61
SSP3-7.0	1.70	1.74	1.56	1.71	1.79
SSP5-8.5	1.72	1.76	1.57	1.81	1.76

Table 2. Similar to Table 1. but for the Amplification Index eliminating Earth’s three poles mean (PAI2).

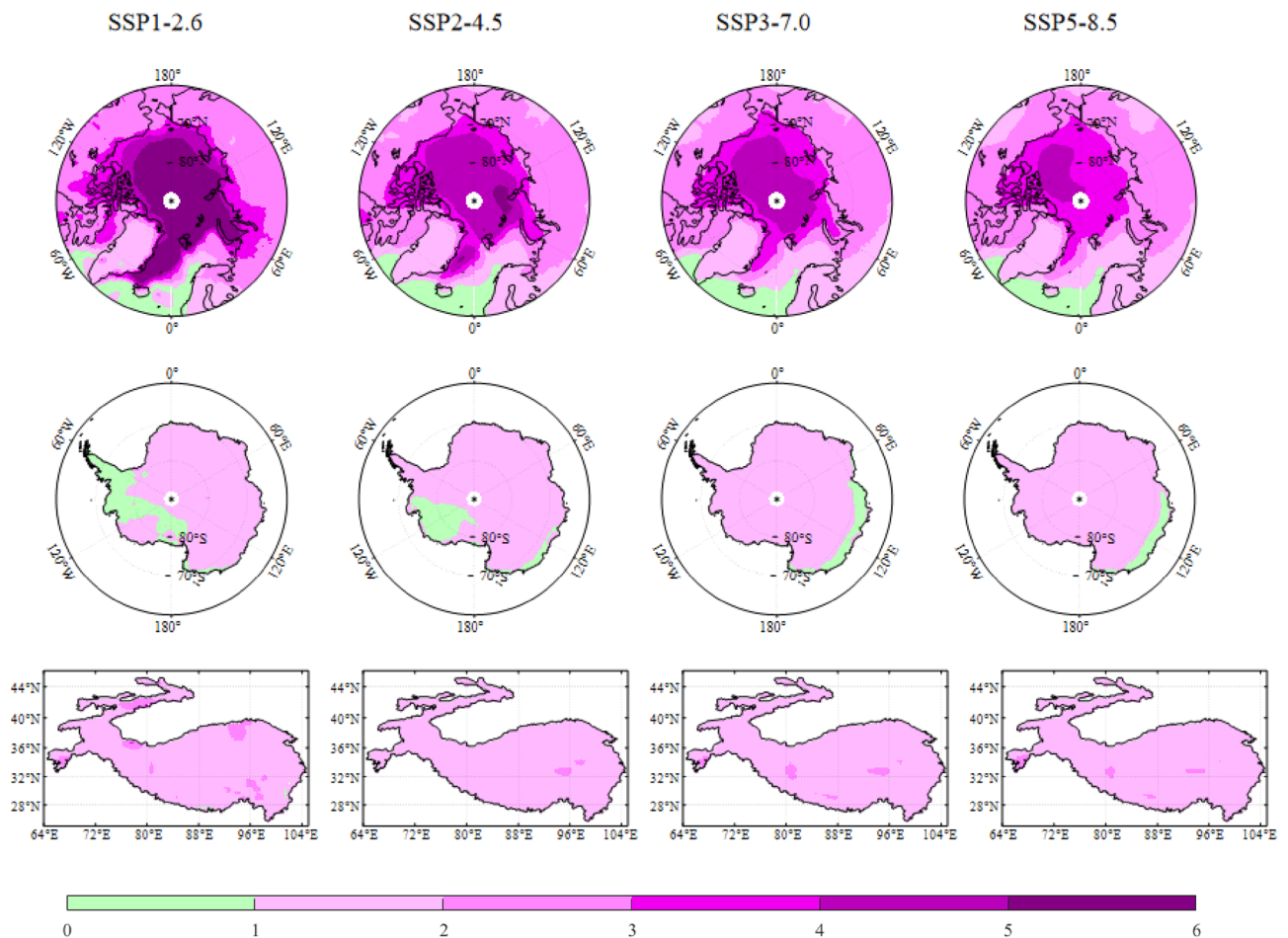


Figure 10. Similar to Fig. 9, but for the PAI2 that eliminating Earth’s three poles. The map was drawn in the software MATLAB R2018b (<https://ww2.mathworks.cn/products/matlab.html>).

autumn⁵⁵. Corresponding to it, the strongest AA appears in these seasons, whereas the sign is weaker in summer⁵⁶, and the characteristics will exist in the near future in all SSPs. The mechanism of AA can be divided into local and remote forcing, and they may interact and boost each other^{24, 57}. Sea ice plays an important role in AA, and the greater absorption of solar radiation in summer can promote anomalous latent and sensible heat fluxes in the autumn. These factors delay sea ice growth in cold seasons, induce the warmer and moister Arctic air masses

into Arctic, and accelerate the conspicuous AA in autumn and winter⁵⁸. In addition, the warming cloud feedback also influences the fast warming⁵⁹. Strong positive ice-temperature feedbacks increase the chances of further rapid warming¹³, and it indicates the greater AA may appear. In JJA, the increase of the absorbed shortwave radiation is very much dictated offset by the greater sea ice loss in Arctic³³. The tropospheric-mean atmospheric warming and greenhouse gas increases for tropical and Arctic regions contribute to the Arctic amplification, in addition, non barotropic and surface warming sensitivity effects also accelerates the amplification⁴⁴. However, CMIP5 models hold the point that changes in downward longwave radiation flux from a cloudless atmosphere is the major factor affecting the AA⁶⁰. Research on the future AA provides that ocean coupling is responsible for AA during the twenty-first century, mostly via thermodynamic coupling⁶¹.

The projected changes over the coastal areas of Antarctica do not match linearly with global forcing. Compared with the high forcing, the warming over the coastal Antarctica is stronger in the low forcing relative to the global mean⁶². In SSP3-7.0 and SSP5-8.5, the warming over the East Antarctica ice sheet (EAIS) is conspicuous. EAIS is highly sensitive to ocean forcing for the geometries and connectivity to the Southern Ocean, and the southerly shifts of Southern Hemisphere Westerlies may induce the general warming⁶³. EAIS performs a dynamic response to the continued anthropogenic warming, and its contribution to future global sea-level may be underestimated⁶⁴, and it is more obvious reflected in the conspicuous warming signal in CMIP6. When different RCP scenarios and thresholds are selected, there are great differences between atmosphere and sea ice, and keeping global warming below 1.5°C has a significant impact on the distribution of sea ice in the Southern Ocean⁶⁵. Over Antarctica, the greatest amplification occurs in austral autumn MAM. Increased poleward moisture transport is the largest contributor to projected Antarctic warming, and seasonal ocean heat storage contribute a winter peak⁶⁶, and it relates to the weaker AnA in winter than in autumn. Among the Earth's three poles, Antarctic amplification is the weakest in general. Firstly, Southern Ocean is the crucial factor for the huge accumulated ocean heat uptake⁷. Secondly, the high elevation of Antarctica plays an important role in decreasing the susceptibility to CO₂-forced warming⁶⁷.

In recent decades, especially at the beginning of the twenty-first century, the Tibetan Plateau (TP) has been experiencing a more rapid warming than its surrounding regions⁶⁸. The CMIP5 MEM has found that the warming amplification in high altitude regions of the northern hemisphere is greater in higher greenhouse gas emission scenario⁶⁹. The amplification of the Third Pole is conspicuous in the different scenarios in CMIP5, and the warming rate might make an obvious discrepancy to the future amplification at different thresholds²⁰. The Third Pole amplification continues to exist in CMIP6, and becomes stronger in the higher forcing scenario. Altitude and latitude both contribute to the warming of the Third Pole, and the snow albedo feedback also plays an important role in the Third Pole warming amplification⁷⁰. In addition, the enhancement of downward clear-sky longwave radiative fluxes and surface albedo feedback also promote the accelerated warming⁷¹. So far, there is no evidence that the Third Pole amplification relates to global circulation changes, and the mechanisms focus on the local to the mountain ranges²⁷.

Conclusions

This study provides the initial evaluation on amplification comparison of Earth's three poles surface temperature variations from 1850 to 2100 based on the CMIP6 multi-model outputs under five socioeconomic pathways of SSP1-1.9, SSP1-2.6, SSP2-4.5, SSP3-7.0 and SSP5-8.5. The main results are summarized as the following.

(1). Among Earth's three poles, Arctic displays the most conspicuous warming, followed by the Third Pole, and Antarctica generally shows the weakest warming. The warming trend over Earth's three poles will enhance with the increase of forcing from low emissions scenario SSP1-1.9 to high emissions scenario SSP5-8.5.

(2). Arctic shows the strongest warming in winter, The Third Pole shows the most conspicuous in autumn. Similarly to Arctic, the Antarctic temperature exhibits the characteristic of the highest warming in austral winter. Under SSP5-8.5, the warming trend is 1.55 °C, 0.84 °C and 0.65 °C per decade over Arctic, The Third Pole and Antarctica, respectively.

(3). When global warming exceeds from 1.5 °C to 2.0 °C thresholds, Arctic annual temperature increases higher than 0.85 °C under all socioeconomic scenarios. The Third Pole also warms higher than the global mean, but lower than Arctic except in summer. Differently, Antarctica warms always lower than 0.5 °C except in SSP1-2.6.

(4). When global warming of 2.0 °C to 3.0 °C, the increase of Arctic annual temperature exceeds 2.3 °C, with the warming more than 3.0 °C in winter under all scenarios. However, Antarctica fails to warm 1.0 °C in most cases. The Third Pole also follows Arctic with the annual warming higher than 1.3 °C.

(5). AA always occurs, with the weakest amplification (PAI1 > 1.34) in summer, and the strongest (PAI1 > 2.73) in winter under different socioeconomic scenarios. For the Third Pole, the amplification is strong in summer (PAI1 > 1.31) and autumn (PAI1 > 1.09). AnA only occurs in SSP5-8.5, with the annual PAI1 of 1.03. In SSP3-7.0 and SSP5-8.5, the slightly AnA occurs in austral autumn (PAI1 > 1.16) and winter (PAI1 > 1.09). The AA intensity becomes weak with the increase of forcing, whereas the Antarctica and the Third Pole show the reverse phenomenon. This demonstrates that the rate of future warming might make a large difference from nowadays among Earth's three poles under different scenarios.

(6). To eliminate the self-influence from Earth's three poles warming, this study has especially defined one other new PA index (PAI2). The result shows that the amplification enhances obviously over Earth's three poles under different scenarios, especially for Arctic in winter (DJF, PAI2 > 4.08), and even for Antarctica in austral autumn (PAI2 > 1.38). The PA warming over the Earth's three poles is conspicuously faster than the other regions of global mean through the whole years in all the scenarios.

This study demonstrates that the rate of future warming might make a large difference from nowadays among Earth's three poles under different scenarios and/or at different thresholds. Our findings call for the separate

contribution from natural variability and anthropogenic forcing. Understanding any differences therein is of vital importance for future adaptation and mitigation strategies over the regions. Despite the greatly improved understanding of spatial and temporal variations of polar amplification, large uncertainties still exist in additional areas of research that require further investigation, especially for Antarctic amplification with scarce research. The uncertainties in polar amplification highlight the importance of further improving the atmosphere and sea ice/snow dynamical and parameterization processes in the state-of-the-art models. The new models will be released in succession, and the more models can be constructive to further improve the estimate accuracy, and to understand well the amplification mechanism over Earth's three poles. Future research needs to further explore the PA vertical profiles with remote sensing data, and to investigate the variations of temperature extremes over Earth's three poles under different future scenarios, both for better scientific understanding the role of polar amplification playing in climate change and for policy making.

Data availability

Publicly available datasets used in this study are from the CMIP6 website <https://esgf-node.llnl.gov/projects/cmip6/>.

Received: 4 February 2022; Accepted: 22 September 2022

Published online: 03 October 2022

References

1. Qiu, J. China: The third pole. *Nature* **454**, 393–396 (2008).
2. Gao, K. L., Duan, A., Chen, D. L. & Wu, G. X. Surface energy budget diagnosis reveals possible mechanism for the different warming rate among Earth's three poles in recent decades. *Sci. Bull.* **64**, 1140–1143 (2019).
3. Li, X. *et al.* CASEarth Poles: Big Data for the Three Poles. *Bull. Am. Meteorol. Soc.* **101**, 1475–1491 (2020).
4. Zheng, G. *et al.* Increasing risk of glacial lake outburst floods from future Third Pole deglaciation. *Nat. Clim. Chang.* **11**, 411–417 (2021).
5. Cohen, J. *et al.* Recent Arctic amplification and extreme mid-latitude weather. *Nat. Geosci.* **7**, 627–637 (2014).
6. Rintoul, S. R. *et al.* Choosing the future of Antarctica. *Nature* **558**, 233–241 (2018).
7. Meredith, M., M. Sommerkorn, S. Cassotta, C. Derksen, A. Ekaykin, A. Hollowed, G. Kofinas, A. Mackintosh, J. Melbourne-Thomas, M.M.C. Muelbert, G. Ottersen, H. Pritchard, and E.A.G. Schuur, 2019: Polar Regions. In: IPCC Special Report on the Ocean and Cryosphere in a Changing Climate [H.-O. Pörtner, D.C. Roberts, V. Masson-Delmotte, P. Zhai, M. Tignor, E. Poloczanska, K. Mintenbeck, A. Alegria, M. Nicolai, A. Okem, J. Petzold, B. Rama, N.M. Weyer (eds.)]. In press.
8. Dai, A. G., Luo, D. H., Song, M. R. & Liu, J. P. Arctic amplification is caused by sea-ice loss under increasing CO₂. *Nat. Commun.* **10**, 121 (2019).
9. Peng, X. Q., Zhang, T. J., Frauenfeld, O. W., Du, R., Jin H. D. & Mu C. C. A Holistic assessment of 1979–2016 Global Cryospheric Extent. *Earth's Future* **9**, e2020EF001969 (2021).
10. Hofer, S. *et al.* Greater Greenland Ice Sheet contribution to global sea level rise in CMIP6. *Nat. Commun.* **11**, 6289 (2020).
11. IPCC, 2021: Summary for Policymakers. In: Climate Change 2021: The Physical Science Basis. Contribution of Working Group I to the Sixth Assessment Report of the Intergovernmental Panel on Climate Change. Masson-Delmotte, V., P. Zhai, A. Pirani, S.L. Connors, C. Péan, S. Berger, N. Caud, Y. Chen, L. Goldfarb, M.I. Gomis, M. Huang, K. Leitzell, E. Lonnoy, J.B.R. Matthews, T.K. Maycock, T. Waterfield, O. Yelekçi, R. Yu, and B. Zhou (eds.). Cambridge University Press. In Press
12. Chen, J. L., Kang, S. C., Meng, X. H. & You, Q. L. Assessments of the Arctic amplification and the changes in the Arctic sea surface. *Adv. Clim. Chang* **4**, 193–202 (2019).
13. Screen, J. A. & Simmonds, I. The central role of diminishing sea-ice in recent Arctic temperature amplification. *Nature* **464**, 1334–1337 (2010).
14. Bromwich, D. *et al.* Central West Antarctica among the most rapidly warming regions on Earth. *Nat. Geosci.* **6**, 139–145 (2013).
15. Sato, K., Inoue, J., Simmonds, I. & Rudeva, I. Antarctic Peninsula warm winters influenced by Tasman Sea temperatures. *Nat. Commun.* **12**, 1497 (2021).
16. Turner, J. *et al.* Absence of 21st century warming on Antarctic Peninsula consistent with natural variability. *Nature* **535**, 411–415 (2016).
17. Clem, K. R., Renwick, J. A. & McGregor, J. Autumn cooling of Western East Antarctica linked to the Tropical Pacific. *J. Geophys. Res. Atmos.* **123**, 89–107 (2018).
18. Wang, Q., Fan, X. & Wang, M. Recent warming amplification over high elevation regions across the globe. *Clim. Dyn.* **43**, 87–101 (2014).
19. Cai, S. L., Hsu, P. C. & Liu, F. Changes in polar amplification in response to increasing warming in CMIP6. *Atmos. Oceanic Sci. Lett.* **14**, 100043 (2021).
20. You, Q. L. *et al.* Warming amplification over the Arctic Pole and Third Pole: Trends, mechanisms and consequences. *Earth Sci Res* **217**, 103625 (2021).
21. Duan, J. P., Li, L., Chen, L. & Zhang, H. Time-dependent warming amplification over the Tibetan Plateau during the past few decades. *Atmos. Sci. Lett.* **21**, e998 (2020).
22. Fyke, J., Eby, M., Mackintosh, A. & Weaver, A. Impact of climate sensitivity and polar amplification on projections of Greenland Ice Sheet loss. *Clim. Dyn.* **43**, 2249–2260 (2014).
23. Bustos Usta, D. F. & Torres Parra, R. R. Ocean and atmosphere changes in the Caribbean Sea during the twenty-first century using CMIP5 models. *Ocean Dyn* **71**, 757–777 (2021).
24. Hahn, L., Armour, K., Battisti, D., Donohoe, A., Pauling, A. G. & Bitz, C. Antarctic elevation drives hemispheric asymmetry in polar lapse rate climatology and feedback. *Geophys. Res. Lett.* **47**, e2020GL088965 (2020).
25. Stuecker, M. F. *et al.* Polar amplification dominated by local forcing and feedbacks. *Nat. Clim. Chang.* **8**, 1076–1081 (2018).
26. Pithan, F. & Mauritsen, T. Arctic amplification dominated by temperature feedbacks in contemporary climate models. *Nat. Geosci.* **7**, 181–184 (2014).
27. Eyring, V. *et al.* Overview of the coupled model intercomparison project phase 6 (CMIP6) experimental design and organization. *Geosci Model Dev* **9**, 1937–1958 (2016).
28. Forster, P. M., Maycock, A. C., McKenna, C. M. & Smith, C. J. Latest climate models confirm need for urgent mitigation. *Nat. Clim. Chang.* **10**, 7–10 (2020).
29. O'Neill, B. C. *et al.* The roads ahead: Narratives for shared socioeconomic pathways describing world futures in the 21st century. *Glob. Environ. Change* **42**, 169–180 (2017).
30. Roussel, M. L., Lemonnier, F., Genthon, C. & Krinner, G. Brief communication: Evaluating Antarctic precipitation in ERA5 and CMIP6 against CloudSat observations. *Cryosphere* **14**, 2715–2727 (2020).

31. Yao, T. D. Changes and countermeasures of pan third pole environment. *Bull. Chin. Acad. Sci.* **33**, 44–46 (2018).
32. Taylor, K. E., Stouffer, R. J. & Meehl, G. A. An overview of CMIP5 and the experiment design. *Bull. Am. Meteorol. Soc.* **93**, 485–498 (2012).
33. Graham, R. M., Hudson, S. R. & Maturilli, M. Improved performance of ERA5 in Arctic gateway relative to four global atmospheric reanalyses. *Geophys. Res. Lett.* **46**, 6138–6147 (2019).
34. Zhu, J. P., Xie, A. H., Qin, X., Wang, Y. T. & Wang, Y. C. An assessment of ERA5 reanalysis for Antarctic near-surface air temperature. *Atmosphere* **12**, 217 (2021).
35. Han, Y. *et al.* Analysis of wind-speed profiles and optical turbulence above Gaomeigu and the tibetan plateau using ERA5 data. *Mon. Not R. Astron. Soc.* **4**, 4692–4702 (2021).
36. Wilks, D. *Statistical methods in the atmospheric sciences*. Academic Press, 2006.
37. Barnes, E. A. & Polvani, L. M. CMIP5 projections of Arctic amplification, of the North American/North Atlantic circulation, and of their relationship. *J. Clim.* **28**, 5254–5271 (2015).
38. You, Q. L. *et al.* Tibetan Plateau amplification of climate extremes under global warming of 1.5°C, 2°C and 3°C. *Glob. Planet Change* **192**, 103261 (2020).
39. UNFCCC. Adoption of the Paris Agreement. 1–32Paris (2015).
40. Donnelly, C. *et al.* Impacts of climate change on European hydrology at 1.5, 2 and 3 degrees mean global warming above preindustrial level. *Clim. Change* **143**, 13–26 (2017).
41. King, A., Karoly, D. & Henley, B. Australian climate extremes at 1.5 °C and 2 °C of global warming. *Nat. Clim. Chang.* **7**, 412–416 (2017).
42. Hu, X. M., Ma, J. R., Ying, J., Cai, M. & Kong, Y. Q. Inferring future warming in the Arctic from the observed global warming trend and CMIP6 simulations. *Adv. Clim. Change Res.* **12**, 499–507 (2021).
43. Sonali, P. & Nagesh Kumar, D. Review of trend detection methods and their application to detect temperature changes in India. *J. Hydrol* **476**, 212–227 (2013).
44. Lambert, F. *et al.* The role of mineral-dust aerosols in polar temperature amplification. *Nat. Clim. Chang.* **3**, 487–491 (2013).
45. Mahlstein, I. & Knutti, R. Ocean heat transport as a cause for model uncertainty in projected Arctic Warming. *J. Clim.* **24**, 1451–1460 (2011).
46. Sledd, A. & L'Ecuyer, T. Uncertainty in forced and natural Arctic solar absorption variations in CMIP6 models. *J. Clim.* **34**, 1–53 (2020).
47. Roach, L. A. *et al.* Antarctic Sea Ice area in CMIP6. *Geophys. Res. Lett.* **47**, 086729 (2020).
48. Shu, Q. *et al.* Assessment of sea ice extent in CMIP6 with comparison to observations and CMIP5. *Geophys. Res. Lett.* **47**, 2020GL087965 (2020).
49. Gao, M. N. *et al.* Historical fidelity and future change of Amundsen Sea Low under 1.5°C–4°C global warming in CMIP6. *Atmos Res* **255**, 105533 (2021).
50. Zhu, Y. & Yang, S. N. Evaluation of CMIP6 for historical temperature and precipitation over the Tibetan Plateau and its comparison with CMIP5. *Adv. Clim. Chang* **11**, 239–251 (2020).
51. Lun, Y. R., Cheng, L., Li, X. P., Li, H. & Xu, Z. X. Assessment of GCMs simulation performance for precipitation and temperature from CMIP5 to CMIP6 over the Tibetan Plateau. *Int. J. Climatol.* **41**, 7055 (2021).
52. Wang, M. R. *et al.* Recent recovery of the boreal spring sensible heating over the Tibetan Plateau will continue in CMIP6 future projections. *Environ. Res. Lett.* **14**, 124066 (2019).
53. Casagrande, F., Neto, F. A. B., de Souza, R. B. & Nobre, P. Polar amplification and ice free conditions under 1.5, 2 and 3 °C of global warming as simulated by CMIP5 and CMIP6 models. *Atmosphere* **12**, 1494 (2021).
54. You, Q. L., Zhang, Y. Q., Xie, X. & Wu, F. Robust elevation dependency warming over the Tibetan Plateau under global warming of 1.5 °C and 2 °C. *Clim. Dyn.* **53**, 2047–2060 (2019).
55. Koenigk, T. *et al.* Arctic climate change in 21st century CMIP5 simulations with EC-Earth. *Clim Dyn* **40**, 2719–2743 (2013).
56. Francis, J. A. & Vavrus, S. J. Evidence linking Arctic amplification to extreme weather in mid-latitudes. *Geophys. Res. Lett.* **39**, 2012GL051000 (2012).
57. Cohen, J. *et al.* Divergent consensuses on Arctic amplification influence on midlatitude severe winter weather. *Nat. Clim. Chang.* **10**, 20–29 (2020).
58. Pithan, F. *et al.* Role of air-mass transformations in exchange between the Arctic and mid-latitudes. *Nat. Geosci.* **11**, 805–812 (2018).
59. Lainé, A., Yoshimori, M. & Abe-Ouchi, A. Surface Arctic amplification factors in CMIP5 models: Land and oceanic surfaces and seasonality. *J. Clim.* **29**, 3297–3316 (2016).
60. Boeke, R. C. & Taylor, P. C. Seasonal energy exchange in sea ice retreat regions contributes to differences in projected Arctic warming. *Nat. Commun.* **9**, 5017 (2018).
61. Chemke, R., Polvani, L. M., Kay, J. E. & Orbe, C. Quantifying the role of ocean coupling in Arctic amplification and sea-ice loss over the 21st century. *NPJ Clim. Atmos. Sci.* **4**, 46 (2021).
62. Bracegirdle, T. J. *et al.* Twenty first century changes in Antarctic and Southern Ocean surface climate in CMIP6. *Atmos. Sci. Lett.* **21**, e984 (2020).
63. Fogwill, C. J. *et al.* Testing the sensitivity of the East Antarctic Ice Sheet to Southern Ocean dynamics: Past changes and future implications. *J. Quat Sci* **29**, 2683 (2014).
64. Gulick, S. *et al.* Initiation and long-term instability of the East Antarctic Ice Sheet. *Nature* **552**, 225–229 (2017).
65. Saurral, R. I., Raggio, G. A. & Gulizia, C. N. How could a difference of 0.5°C in global warming modify the mean and extreme climate conditions around Antarctica?. *Int. J. Climatol.* **40**, 6566 (2020).
66. Hahn, L. C., Armour, K. C., Zelinka, M. D., Bitz, C. M. & Donohoe, A. Contributions to polar amplification in CMIP5 and CMIP6 models. *Front. Earth Sci.* **9**, 725 (2021).
67. Singh, H. A. & Polvani, L. M. Low Antarctic continental climate sensitivity due to high ice sheet orography. *NPJ Clim. Atmos. Sci.* **3**, 39 (2020).
68. Chen, D. L. *et al.* Assessment of past, present and future environmental changes on the Tibetan Plateau. *Chin. Sci. Bull.* **60**, 3025–3035 (2015).
69. Rangwala, I., Sinsky, E. & Miller, J. R. Amplified warming projections for high altitude regions of the northern hemisphere mid-latitudes from CMIP5 models. *Environ. Res. Lett.* **8**, 024040 (2013).
70. Wang Q. X., Fan, X. H. & Wang, M. B. Warming amplification with both altitude and latitude in the Tibetan Plateau. *Int. J. Climatol.* **1–18** (2021).
71. Su, J., Duan, A. & Xu, H. Quantitative analysis of surface warming amplification over the Tibetan Plateau after the late 1990s using surface energy balance equation: Tibetan Plateau warming amplification. *Atmos. Sci. Lett.* **18**, 112–117 (2017).

Acknowledgements

This work was supported by the Chinese Academy of Sciences (131B62KYSB20180003, QYZDY-SSW-DQC021), the second Tibetan Plateau Scientific Expedition and Research Program (STEP) (2019QZKK020103), and the National Natural Science Foundation of China (41671073, 42276260). We gratefully acknowledge the Coupled Model Intercomparison Project who supplied the data used in this study.

Author contributions

A.X.: Writing—Original Draft, Conceptualization, Formal analysis. J.Z.: Writing—Review & Editing, Conceptualization, Methodology, Software. S.K.: Writing—Review & Editing. X.Q.: Writing—Review & Editing. B.X.: Visualization, Software. Y.W.: Data Curation, Software.

Competing interests

The authors declare no competing interests.

Additional information

Supplementary Information The online version contains supplementary material available at <https://doi.org/10.1038/s41598-022-21060-3>.

Correspondence and requests for materials should be addressed to J.Z.

Reprints and permissions information is available at www.nature.com/reprints.

Publisher's note Springer Nature remains neutral with regard to jurisdictional claims in published maps and institutional affiliations.



Open Access This article is licensed under a Creative Commons Attribution 4.0 International License, which permits use, sharing, adaptation, distribution and reproduction in any medium or format, as long as you give appropriate credit to the original author(s) and the source, provide a link to the Creative Commons licence, and indicate if changes were made. The images or other third party material in this article are included in the article's Creative Commons licence, unless indicated otherwise in a credit line to the material. If material is not included in the article's Creative Commons licence and your intended use is not permitted by statutory regulation or exceeds the permitted use, you will need to obtain permission directly from the copyright holder. To view a copy of this licence, visit <http://creativecommons.org/licenses/by/4.0/>.

© The Author(s) 2022